Architectural analysis and performance evaluation of Integrated Access-Backhaul Non-Terrestrial Networks

Daniele Pugliese
DEI
Politecnico di Bari
Bari, Italy
daniele.pugliese@poliba.it

Mattia Quadrini
DIE
Università di Roma "Tor Vergata"
Rome, Italy
mattia.quadrini@uniroma2.it

Domenico Striccoli
DEI
Politecnico di Bari
Bari, Italy
domenico.striccoli@poliba.it

Giuseppe Piro
DEI
Politecnico di Bari
Bari, Italy
giuseppe.piro@poliba.it

Cesare Roseti
DIE
Università di Roma "Tor Vergata"
Rome, Italy
roseti@ing.uniroma2.it

Gennaro Boggia
DEI
Politecnico di Bari
Bari, Italy
gennaro.boggia@poliba.it

Luigi Alfredo Grieco
DEI
Politecnico di Bari
Bari, Italy
alfredo.grieco@poliba.it

***Abstract*—The growing attention devoted to the wireless backhauling and relaying capabilities of 5G networks, and the related satellite link integration is testified in the latest releases of 3GPP 5G standards. Both these aspects are essential to guarantee interoperability and integration of relays from different vendors, as well as to benefit from the economies of scale of 3GPP technologies by satellite ecosystems, lowering costs of 5G network implementations and satellite connectivity. Nevertheless, the adoption of a satellite link characterizing the non-terrestrial network implies a series of issues and protocol adaptations, mainly due to the high propagation delay. This holds true especially for the backhaul link, that must guarantee service continuity, reliability, and availability. There have been some studies in the recent past that analyzed the protocol adaptations needed for a satellite link, but they were conducted in the context of 4G networks, and only for the access network. To bridge this gap, this paper analyzes 5G non-terrestrial networks with satellite backhaul links, proposing some key architectures and the related protocol adaptations. A satellite link analysis and a system-level throughput evaluation are also carried out in some reference scenarios, considering the most recent 5G-related aspects to assess the effective utilization of satellites in new integrated terrestrial-satellite network scenarios.**

***Index Terms*—Architectural Analysis, Integrated Access-Backhaul, Link-level Analysis, Non-Terrestrial Network, System-level Evaluation.**

I. Introduction

One of the most important evolution paths in the Next Generation Radio Access Network (NG-RAN) architectures proposed by Third Generation Partnership Project (3GPP) includes two significant enhancements: the adoption of relaying, which is also referred to as Integrated Access Backhaul (IAB), and the implementation of satellite (access and backhaul) links, that translates into the concept of the so-called Non Terrestrial Networks (NTNs) [1]. The most relevant aspect of IAB is to reduce the adoption of fiber-based backhauling among different cells of a network, by exploiting wireless backhauling to the next fiber-connected point. Furthermore, the integration with the wireless access network allows to increase the efficiency in spectral resource utilization, reducing costs and reaching target performance guarantees [1], [2].

Traditionally, 3GPP networks have been designed to support almost exclusively terrestrial mobile networks. On the contrary, Fifth-Generation (5G) standardization efforts are currently dedicated to satellite-based scenarios. Studies in this direction have been conducted starting from Release-15, which introduced only a few specific cases and scenarios, and are still under development in Release-17 to fully support a wider variety of NTN scenarios [3].

Nevertheless, the adoption of NTN in the design of 5G networks implies a series of issues and adaptations at different layers of the protocol stack to account for the much higher propagation delays in the satellite link. They involve the modification of various timers, the Random Access CHannel (RACH) and Hybrid Automatic Repeat reQuest (HARQ) procedures, and the high Doppler shift in the case of Low Earth Orbit (LEO) satellites [4]. These adaptations and issues are even more critical if the satellite link is a backhaul link, since service continuity, reliability, and availability must be guaranteed in all the parts of the network, across the different relay nodes, which is a pillar of IAB networks.

There are some studies proposed in the recent past that analyze the adaptations described above and needed for NTNs [5], [6]. Nevertheless, they all refer to the access network, and are tailored for the NarrowBand Internet of Things (NB-IoT) standard. So, it is very important to extend the applicability and feasibility of IAB network architectures, in which satellite links feed both the access and backhaul, as well as to analyze the satellite link connectivity in such architectures, while taking into account the most recent 5G specifications. With all this in mind, the goal of this contribution is threefold. First, it aims at describing the most representative architectural options of IAB NTNs, motivating the selection of the most suitable one with the related adaptations. Second, it proposes a performance analysis of the satellite link, that can act as access or backhaul

link, also evaluating the link performance in terms of data rate. Third, some considerations at system level are drawn, concerning the resource splitting and throughput analysis.

The remainder of the paper is structured as follows. Section II provides an overview of the IAB NTN architectures. Section III focuses on one selected architecture, describing the adaptations at different protocol layers. Section IV provides a performance analysis for the satellite link at physical and link layers. Section V analyzes some aspects of the system-level performance. Finally, Section VI concludes the work.

II. Overview of IAB NTN architectures

The IAB technology has been defined in Rel-16 and enhanced in the current Rel-17 [7]. The main goal is to reuse radio resources to extend the radio coverage in both the access and backhaul networks. An IAB network consists of a set of "IAB nodes" under the control of an "IAB donor" representing the end-point of the Radio Access Network (RAN) connected directly to the 5G Core (5GC) network. The IAB node implements a dual stack: the Distributed Unit (DU), to handle communications in the access network towards User Equipment (UE) and acting as a 5G Node B (gNB); the Mobile Termination (MT), to handle communications in the backhaul towards parent DU and acting as a UE. The IAB donor implements a Central Unit (CU) stack, to control all IAB node's DUs in the network (i.e., initialization, setup and configuration), and to manage communications to the 5GC. Communications in the backhaul are supported by a 3GPP-defined adaptation layer, the so-called Backhaul Adaption Protocol (BAP) [8].

An IAB network by definition can consist of multiple nodes supporting a variety of topologies. But in general, a multi-hop topology could cause congestion at the network level already at the first hop. In a topology made up by Terrestrial and Non-Terrestrial nodes, the presence of the satellite can reduce the dimension and the load of the IAB network, because the donor can be reached with a single hop bypassing the terrestrial nodes.

The architecture of the satellite system impacts the IAB NTN topology in terms of role (whether node or donor), operating frequency bands (whether L/S band in FR1 or Ka/Q/V band in FR2), and band management configuration (whether In-Band or Out-of-Band). The orbit selection represents the main critical aspect. The Non-Geostationary Orbit (NGSO) satellite is characterised by continuous movement, and it cannot guarantee the service continuity over time, unless a constellation of satellites with Inter-Satellite Link (ISL) support is designed [9]. However, this configuration benefits from a lower latency and a smaller propagation loss compared to Medium-Earth Orbit (MEO) and Geostationary Orbit (GEO) satellites.

A. NTN topology options

In general, two macro-architectures can be delineated, that consider the satellite as an IAB node or as an IAB donor. Based on this macro-categorisation, a number of NTN topologies options for IAB are proposed below in which the satellite can represent an added value.

1) Option 1: A single satellite implements a IAB node protocol stack and represents the last hop to reach the terrestrial IAB donor. Basically, it manages the backhauling from child nodes to the donor, both on the ground, allowing to minimize the distance from the 5GC and thus reducing the latency on the interfaces. Donor-node connectivity must be guaranteed over time to achieve service continuity which represents a critical aspect for LEO. The latency of the RAN significantly increases much beyond the 5G requirements, making the IAB system applicability limited to a small number of 5G services. More in general, the performance on the end-to-end data transfers are degraded, especially in harsh communication conditions (i.e. fading, rain, terrestrial mobility) due to retransmissions and/or re-ordering operations.

2) Option 2: All the IAB nodes are installed on a satellite constellation communicating with the IAB donor on the ground, intrinsically ensuring service continuity. The support for ISL is needed and ensures connectivity between satellite IAB nodes towards the IAB donor on the ground. This option simplifies the terrestrial IAB configuration, making IAB service accessible theoretically worldwide with a full LEO constellation. In turn, the backhauling is fully managed in satellite domain. Then, the bottleneck is moved at the access link between NTN-UE and satellite IAB node. In fact, the service is mainly limited to this terminal typology. Routing is then the major issue to make system efficient. The BAP must be enhanced in order to consider satellite ephemeris and the coordinates of the IAB node.

3) Option 3: The IAB donor is installed on board the satellite and serves child IAB nodes on the ground. The network connection between the satellite and the NTN Gateway is required over the time to guarantee communication toward the 5GC. Eventually, a satellite constellation can be assumed making available multiple satellite IAB donors (i.e., multiple CUs, one per satellite) to guarantee resiliency with DUs, as foreseen by the 3GPP in the specification 38.401 [10].

4) Option 4: The IAB network is fully deployed on a satellite constellation including the satellite IAB donor. As a matter of fact, this option merges Option 2 and Option 3, resulting into an equivalent gNB on the space potentially covering user spread worldwide. Thus, support for ISL is mandatory, and any New Radio (NR) communication management issue on ISL must be addressed. Being entirely on the space, IAB with this configuration can overcome 3GPP constraints in terms of frequency bands and duplexing scheme.

III. Selected architecture and adaptations

The introduction of the satellite segment in a distributed gNB system will require adaptations at higher layer protocols, i.e., Radio Link Control (RLC) and Packet Data Convergence Protocol (PDCP). The PDCP timers handled by UEs are affected by the end-to-end delay which increases as the number of IAB nodes (hops) increase. Moreover, satellite delays

affect also the initial procedures, as well as subsequent radio reconfiguration and handover operations in case the UE moves to another IAB-DU. In particular, the visibility time in the case of LEO constellations is a worsening factor. Nonetheless, the number of hops can drastically decrease in case of satellite deployment while the one-way latency is in the order of tens of milliseconds.

A. Higher layer adaptations and considerations

Concerning RLC communication, the *T-Reassembly* timer, which is in charge to reconstruct the RLC Protocol Data Unit (PDU) in a given period of time, may be extended adopting the *T-ReassemblyExt*. This parameter can be configured for all UEs and IAB-MT parts served by the satellite IAB donor. Two main timers are defined at PDCP layer: the *discardTimer*, and the *T-Reordering*. The former defines the time after which the buffer of a transmitting PDCP entity is emptied. An extended value is defined by the *DiscardTimerExt2-r17* for this kind of scenario. The *T-Reordering* is used to reconstruct a PDCP packet from RLC segments. In case the timer expires all collected PDCP frames are passed to the upper layer and the reception window will be updated to receive the next packet. Eventually, the UE can set this value to infinity.

Both RLC and PDCP base the transmission and reception of packets on a sliding window. In NR, the receiving window is updated according to different criteria. Considering the RLC Acknowledged Mode (AM), the receiving window is updated in case of in-order delivery or when all missing PDUs are correctly recovered. On the contrary, at PDCP layer the window is updated in case of in-order delivery or when *T-Reordering* expires. This independent management of the receiving windows causes a misalignment problem as discussed in [11]. This leads to an inefficiency, because packets recovered at RLC layer are then discarded by PDCP since they fall outside the PDCP receiving window. Therefore, a suitable configuration of these timers is required taking into account the overall end-to-end delay.

B. Satellite IAB-donor

The list of architectures presented in Section II aims to facilitate the integration of satellite into an IAB topology. This work focuses on a hybrid approach that assumes a satellite equipped with a IAB-donor (topology Option 3) as illustrated in Fig.1. The satellite IAB-donor (DU part) manages links with either ground IAB nodes (backhaul) and NTN UEs (access) using the same NTN-NR interface. The main difference, with respect to the other solutions, is that satellite connection to the NTN Gateway towards 5GC is via NG interfaces, then possibly leveraging satellite technology out of the IAB perimeter. In fact, gNB functionalities are just spread on the ground IAB node and satellite, and the latter includes also CU part. As a straightforward consequence the latency in the RAN is halved, with respect to the satellite IAB node configuration, and PDCP connections terminate on board the satellite. The IAB donor on board the satellite is particularly attractive to represent an anchor for possible IAB nodes to be installed on demand and create cost-effective 5G bubbles. NGSO systems require the deployment of multiple CUs (which is envisaged by the 3GPP to guarantee resiliency) and the management of handover operations between IAB-node on the ground and the new IAB-donor (ISL is required). In particular, the handover is intended between the DU-part of the IAB-node and the CU-part of the IAB-donor, and between the MT-part of the IAB-node and DU-part of the IAB-donor. It is noteworthy that this aspect is not actually covered by 3GPP.

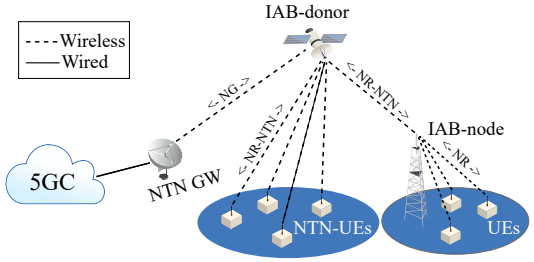

Fig. 1. Satellite-donor IAB architecture in detail.

IV. Link-level analysis

According to what described in Section III, the most critical part of the selected architecture is the satellite link integrated into the IAB network. The goal of this section is to investigate the performance of the wireless link between the ground and the satellite nodes. The considered radio access technology is NR, whose reference values, where standardised, are used in the link-level analysis that follows.

A. Reference scenarios

In order to carry out a comprehensive analysis of NTN architectures enabled by the IAB technology, the three scenarios shown in Figure 2 have been considered. In particular, Fig. 2(a) represents a direct satellite access between a terrestrial UE and a satellite gNB, considered as a benchmark. In Fig. 2(b) a Unmanned Aerial Vehicle (UAV) performs the function of an IAB-node backhauling to a satellite IAB-donor. This can be considered as a possible solution for urban scenarios with a high presence of obstacles. Finally, in Fig. 2(c) terrestrial nodes communicate with a Base Station (BS) which in turn backhauls data to the satellite IAB-donor.

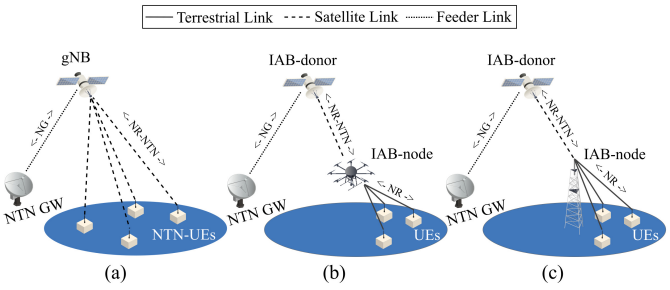

Fig. 2. Overview of the reference scenarios for link-level analysis.

Regarding the non-terrestrial part of the architecture, a LEO satellite with an orbital height of $600\,\mathrm{km}$ has been chosen. The Doppler shift has not been considered in this analysis, as it can be compensated by knowing with good accuracy the relative satellite-ground position through Global Navigation Satellite System (GNSS) techniques and satellite ephemeris at UE side [12]. The main parameters employed in the link-level simulations are given in Table I, if not otherwise specified. More specifically, in Table I the configurations of the satellite antennas are labeled as *SAT* (followed by a reference number), while the configurations of the ground BS antennas are labeled as *BS* (again, followed by a reference number).

The *SAT1* configuration of Table I is considered in the study because it is usually mandatory for small satellites [5]. The UAV antenna and *BS1* configuration are chosen to be coherent in size with the platform on which they are installed. The *SAT2* configuration is fully derived from [4], which also contains indications on the antenna configurations for both the UE and satellite nodes. Finally, the *BS2* and *SAT3* configurations reflect the parameters adopted in [13] and are considered as benchmark.

Starting from the scenarios depicted in Figure 2 and the parameters reported in Table I, the following setups have been considered for link-level simulations:

- A UE communicating with the satellite, which in turn is equipped with *SAT1*, *SAT2* or *SAT3* antenna configurations;
- A UAV establishing a satellite link with *SAT1* or *SAT2* as the receiving configuration;
- A BS, which employs *BS1* configuration when *SAT1* or *SAT2* is used on board the satellite, or *BS2* in conjunction with *SAT3*;
- A BS equipped with *BS1*, capable of tracking the position of the satellite (i.e., pointing), itself equipped with *SAT1* or *SAT2*.

TABLE I
ADOPTED PARAMETER SETTINGS FOR LINK-LEVEL SIMULATIONS.

Parameter	**Value**	**Parameter**	**Value**
Carrier frequency	2 [GHz]	Satellite Noise Figure	5 [dB]
Bandwidth	$12 \times SCS$ with $SCS = 15$ [kHz]	UE, UAV, BS Power	23, 38, 38 [dBm]
UE, UAV antenna	Omni-directional antenna, linear polarization	Sat. antenna configuration 1 (*SAT1*)	Circular patch with a maximum gain of 7 dBi
BS antenna configuration 1 (*BS1*)	Parabolic reflector with a maximum gain of 24 dBi	Sat. antenna configuration 2 (*SAT2*)	Parabolic reflector with a maximum gain of 30 dBi
BS antenna configuration 2 (*BS2*)	Parabolic reflector with a maximum gain of 32.8 dBi	Sat. antenna configuration 3 (*SAT3*)	Parabolic reflector with a maximum gain of 36 dBi

B. Link Budget and SNR analysis

The first phase aims to calculate the link budget of the satellite link to derive the received Signal to Noise Ratio (SNR) value in both uplink and downlink directions. In this study, only results in the uplink direction are provided, being the uplink the most critical direction of the communication. The method adopted is based on what is described in [14] and [15], using theoretical formulations to model real phenomena that degrade signal quality. In particular, the SNR has been calculated for different elevation angles of the satellite (i.e., θ_{el}). This angle directly impacts on the channel impairments, i.e., the antenna diagram correction factors, the free space path loss, and losses due to the medium characteristics, scintillation, and cross-polarization.

Figure 3(a) illustrates the results obtained when the NTN terminal is a UE or a UAV. As obvious, the link performance in case of the UAV adoption are better if compared to UE, in all the configuration scenarios. Moreover, *SAT1* performs better for small angles than *SAT2* and *SAT3*, reaching a peak of $2.16\,\mathrm{dB}$ when the terminal is a UAV.

Nevertheless, the relatively low SNR values obtained ($2.16\,\mathrm{dB}$ at $\theta_{el} =\sim 90°$) in general discourage the adoption of the *SAT1* configuration. On the other hand, *SAT2* and *SAT3* configurations reach higher SNR values starting from $\theta_{el} =\sim 80°$ on, if compared to *SAT1*. As can be seen by Figure 3(a), in the case of a UE transmitting towards the satellite, *SAT2* performs $\sim 6\,\mathrm{dB}$ worse than *SAT3*. In general, the highest SNR values are obtained if a UAV transmits towards the satellite with the *SAT2* configuration, reaching a maximum SNR of $25.37\,\mathrm{dB}$.

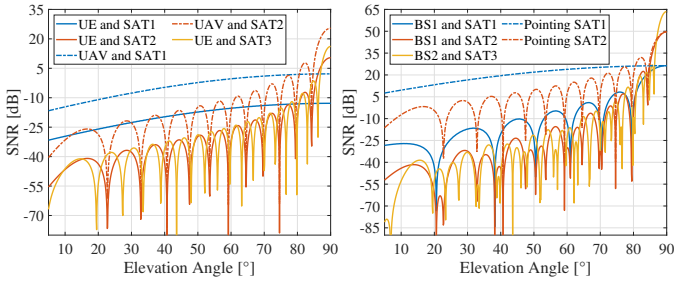

(a) (b)

Fig. 3. SNR for (a) UE, UAV and (b) BS, for different antenna configurations.

Figure 3(b) illustrates the results obtained for the scenario in which the NTN terminal is a BS. Regarding configurations in which pointing is performed (i.e. *BS1* tracking satellite position), it can be noted that *SAT1* maintains a more stable SNR than *SAT2*, reaching good values as soon as $\theta_{el} = 5°$. A similar consideration can be made when adopting *BS1* without pointing. In particular, the behavior in the last $10°$ is more linear for *SAT1*, but reaches a higher value ($49.5\,\mathrm{dB}$) for *SAT2*. Finally, the *BS1*/*SAT2* combination taken from the standards and proposed in this work, reaches lower maximum values than the *BS2* and *SAT3* combo of [13].

C. Data rate evaluation

Starting from the SNR results, and through the adoption of the MATLAB 5G Toolbox [16], this second phase aims to evaluate the achievable data rate on the radio interface employing NR technology. Again, the study focuses on the uplink direction. Since SNR varies in a wide range of values, an Adaptive Modulation and Coding (AMC) mechanism has

been implemented [17]. To this end, BLock Error Rate (BLER) curves have been derived and adopted to establish thresholds above which a certain Modulation and Coding Scheme (MCS) can be used with a decoding error lower than 10%, The rate calculation has been done by considering the ratio between Transport Block Size (TBS) and slot duration. The former is calculated according to what stated in [17], assuming 13 symbols per slot, 6 symbols per Phisical Resource Block (PRB) for DeModulation Reference Signal (DMRS) and 0 symbols of overhead. The latter has been set equal to 1 ms, in accordance to the numerology for $SCS = 15$ kHz.

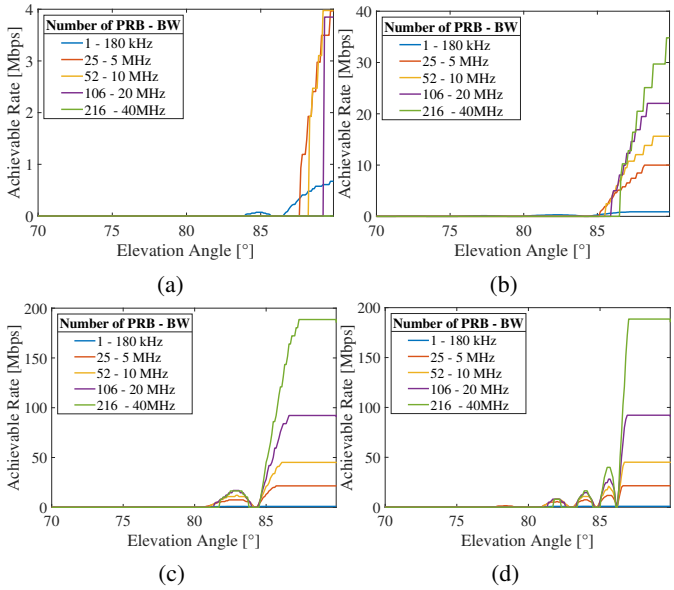

Fig. 4. Achievable Rate when pointing is not performed, for different elevation angles. The combination of transmitter and satellite configuration are (a) UE to *SAT3*, (b) UAV to *SAT2*, (c) *BS1* to *SAT2* and (d) *BS2* to *SAT3*.

Figure 4 shows the results for some of the most interesting configurations when the ground node antenna has a fixed orientation and does not follow the satellite trajectory (pointing is not performed). In general, it can be noted how the parabolic antenna allows transmission only for higher elevation angles. Furthermore, in all cases, it can be observed that the greater the bandwidth, the higher the achievable rate. More in detail, the uplink transmission from UE to *SAT3* performs poorly, reaching a maximum of 3.98 Mbps with 20 MHz. On the other hand, when a UAV is transmitting to *SAT2*, the use of 40 MHz is possible from $\theta_{el} =\sim 87°$, with a peak value of 34.81 Mbps. Scenarios in which *BS1* transmits to *SAT2* perform quite similar to *BS2* with *SAT3*, saturating both at 188.576 Mbps, which is the maximum achievable rate with 40 MHz and the NR-compliant setup adopted.

Results shown in Figure 5, instead, refer to the case in which the ground node antenna in the *BS1* configuration follows the satellite trajectory, i.e., antenna pointing is performed. The satellite configurations considered are *SAT1* and *SAT2*. The first obvious consideration is that, depending on the PRBs assigned, the adoption of *SAT1* allows to transmit for most of the visibility time. However, this comes at a cost of a peak

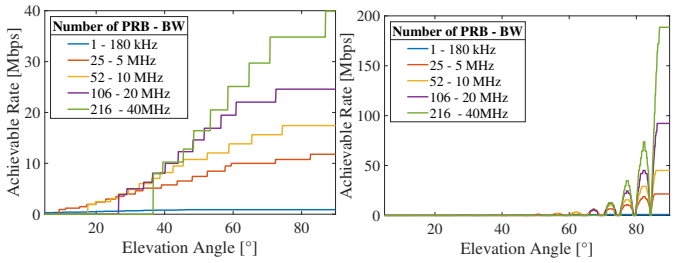

Fig. 5. Achievable Rate when pointing is performed, for different elevation angles. The transmitter is a *BS1* to (a) *SAT1* and (b) *SAT2*.

rate of 39.94 Mbps, which is lower if compared to *SAT2*. For *SAT2* configuration, very high data rates are obtained after $\theta_{el} =\sim 70°$; however, the link is not stable as in the case of *SAT1*.

V. System-level considerations

Following the satellite link analysis, this section proposes some system-level considerations about scenarios (b) and (c) of Figure 2. It is assumed here that the end-to-end performance of an IAB NTN architecture is lower-bounded by the satellite link that constitutes the system bottleneck.

A. Access and backhaul resource splitting

Regarding the configuration of the IAB architecture, an IAB node operating in the in-band mode has been considered, adopting a Time Division Duplex (TDD) solution in which the uplink (downlink) channel on the access side cannot operate simultaneously with the uplink (downlink) channel on the backhaul side. Figure 6 shows the three TDD patterns proposed and adopted in this study, where each block represents a slot (i.e., 1 ms for $SCS = 15$ kHz). Note that a time slot is left idle whenever a switch from access to backhaul and vice versa is needed.

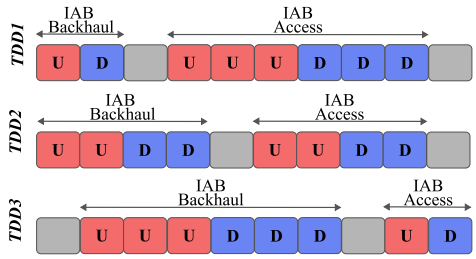

Fig. 6. Proposed TDD patterns.

B. Throughput analysis

For the results proposed here, the time period that the satellite takes from $\theta_{el} = 30°$ to $\theta_{el} = 90°$ and back again to $\theta_{el} = 30°$ has been considered. This trajectory lasts 269 s with the channel conditions varying as a function of the elevation angle. Table II shows the uplink results in terms of average end-to-end throughput, from terrestrial nodes to satellite via IAB. As expected, for all configurations, higher

bandwidth results in higher throughput. Regarding resource splitting, for *TDD1* pattern the satellite link (i.e. backhaul) is active $20\,\%$ of the total time. This time increases to $40\,\%$ for *TDD2* and $60\,\%$ for *TDD3*, increasing in all cases the average throughput as well. Concerning the scenario in which antenna pointing is applied, performance turns out to be higher when *SAT1* is used if compared to *SAT2*. This means that, despite the fact that *SAT2* allows higher data rates for $\theta_{el} = 90°$, the ability to transmit for smaller elevation angles benefits the average throughput and link availability. Moreover, as might be expected, in the case of *SAT2* when pointing is performed throughput results are better than without pointing. Finally, the case in which the UAV relays data to the satellite achieves a throughput of at most $0.50\,\mathrm{Mbps}$. This makes this configuration suitable for scenarios where a high data rate is not required.

TABLE II
AVERAGE THROUGHPUT FOR DIFFERENT TDD PATTERNS AND BANDWIDTHS.

		TDD1	TDD2	TDD3
UAV to *SAT2*	5 MHz	0.07 Mbps	0.15 Mbps	0.22 Mbps
	10 MHz	0.11 Mbps	0.21 Mbps	0.32 Mbps
	20 MHz	0.14 Mbps	0.28 Mbps	0.43 Mbps
	40 MHz	0.17 Mbps	0.33 Mbps	0.50 Mbps
BSI to *SAT2*	5 MHz	0.28 Mbps	0.56 Mbps	0.84 Mbps
	10 MHz	0.54 Mbps	1.08 Mbps	1.62 Mbps
	20 MHz	1.00 Mbps	2.00 Mbps	2.99 Mbps
	40 MHz	1.82 Mbps	3.65 Mbps	5.47 Mbps
Pointing *SAT1*	5 MHz	1.57 Mbps	3.14 Mbps	4.70 Mbps
	10 MHz	2.28 Mbps	4.57 Mbps	6.85 Mbps
	20 MHz	3.07 Mbps	6.14 Mbps	9.20 Mbps
	40 MHz	3.60 Mbps	7.20 Mbps	10.81 Mbps
Pointing *SAT2*	5 MHz	0.59 Mbps	1.18 Mbps	1.77 Mbps
	10 MHz	0.96 Mbps	1.92 Mbps	2.88 Mbps
	20 MHz	1.57 Mbps	3.14 Mbps	4.71 Mbps
	40 MHz	2.61 Mbps	5.23 Mbps	7.84 Mbps

VI. CONCLUSIONS

In this work, some architectural options for IAB NTN have been analyzed, selecting the most suitable one to study the necessary adaptations. Some scenarios compatible with the chosen architecture have been studied, evaluating satellite access in terms of SNR and data rate. The system-level throughput analysis has highlighted some peculiarities regarding each considered configuration scenario.

ACKNOWLEDGEMENTS

This work was partially supported by the European Union under the Italian National Recovery and Resilience Plan (NRRP) of NextGenerationEU, with particular reference to the partnership on "Telecommunications of the Future" (PE00000001 - program "RESTART", CUP: D93C22000910001) and the national center on "Sustainable Mobility" (CN00000023 - program "MOST", CUP: D93C22000410001). It was also supported by the PRIN project no. 2017NS9FEY entitled "Realtime Control of 5G Wireless Networks: Taming the Complexity of Future Transmission and Computation Challenges" funded by the Italian MUR. It was also funded by the European Space Agency, contracts no.4000129810/20/NL/CLP and no.4000139666/22/UK/AL.

REFERENCES

[1] S. Sirotkin, *5G Radio Access Network Architecture: The Dark Side of 5G*. Wiley, 2021.

[2] 3rd Generation Partnership Project, "NR; NR and NG-RAN Overall Description; Stage 2 (Release 17)," TS 38.300, March 2023, [Online; accessed 14-September-2023].

[3] 3rd Generation Partnership Project, "SID for study on solutions for NR to support non-terrestrial networks (NTN)," RP-190710, March 2019, [Online; accessed 14-September-2023].

[4] 3rd Generation Partnership Project, "Solutions for NR to support non-terrestrial networks (NTN)," TR 38.821, April 2023, [Online; accessed 14-September-2023].

[5] G. Sciddurlo, A. Petrosino, M. Quadrini, C. Roseti, D. Striccoli, F. Zampognaro, M. Luglio, S. Perticaroli, A. Mosca, F. Lombardi, I. Micheli, A. Ornatelli, V. Schena, A. D. Mezza, A. Mattioni, D. Morbidelli, G. Boggia, and G. Piro, "Looking at nb-iot over leo satellite systems: Design and evaluation of a service-oriented solution," *IEEE Internet of Things Journal*, vol. 9, no. 16, pp. 14 952–14 964, 2022.

[6] A. Petrosino, G. Sciddurlo, S. Martiradonna, D. Striccoli, G. Piro, and G. Boggia, "Wip: An open-source tool for evaluating system-level performance of nb-iot non-terrestrial networks," in *2021 IEEE 22nd International Symposium on a World of Wireless, Mobile and Multimedia Networks (WoWMoM)*, June 2021, pp. 236–239.

[7] 3rd Generation Partnership Project, "5G; System architecture for the 5G System (5GS)," TS 23.501, July 2023, [Online; accessed 14-September-2023].

[8] 3rd Generation Partnership Project, "NR; Backhaul Adaptation Protocol (BAP) specification," TS 38.340, June 2023, [Online; accessed 14-September-2023].

[9] I. Leyva-Mayorga, B. Soret, M. Röper, D. Wübben, B. Matthiesen, A. Dekorsy, and P. Popovski, "LEO Small-Satellite Constellations for 5G and Beyond-5G Communications," *IEEE Access*, vol. 8, pp. 184 955–184 964, 2020.

[10] 3rd Generation Partnership Project, "5G;NG-RAN; Architecture description," TS 38.401, June 2023, [Online; accessed 14-September-2023].

[11] S. Pandey, R. M. M. K. Eda, and D. Das, "Efficient Reordering-Reassembly PDCP and RLC Window Management Algorithm in 5G and Beyond," in *2020 IEEE International Conference on Electronics, Computing and Communication Technologies (CONECCT)*, July 2020, pp. 1–6.

[12] J. Li, D. Wang, L. Liu, B. Wang, and C. Sun, "Satellite ephemeris broadcasting architecture for 5g integrated leo satellite internet," in *2022 IEEE 22nd International Conference on Communication Technology (ICCT)*, November 2022, pp. 1437–1441.

[13] Z. Abdullah, S. Kisseleff, E. Lagunas, V. N. Ha, F. Zeppenfeldt, and S. Chatzinotas, "Integrated access and backhaul via satellites," in *IEEE International Symposium on Personal, Indoor and Mobile Radio Communications (IEEE PIMRC 2023)*, September 2023, pp. 1–6.

[14] L. Ippolito, *Satellite Communications Systems Engineering: Atmospheric Effects, Satellite Link Design and System Performance*. Wiley, 2017.

[15] 3rd Generation Partnership Project, "Study on New Radio (NR) to support non-terrestrial networks (NTNs)," TS 38.811, October 2020, [Online; accessed 14-September-2023].

[16] "MATLAB 5G Toolbox," https://it.mathworks.com/help/5g/ [Online; accessed 14-September-2023].

[17] 3rd Generation Partnership Project, "Physical layer procedures for data," TS 38.214, June 2023, [Online; accessed 14-September-2023].